Proceedings of the 18th International Conference on Automation & Computing, Loughborough University, Leicestershire, UK, 8 September 2012

Modulation Signal Bispectrum Analysis of Motor Current Signals for Stator Fault Diagnosis

A. Alwodai[1], X. Xia[2], Y. Shao[3*], F. Gu[1], A. D. Ball[1]
[1]Centre for Efficiency and Performance Engineering, University of Huddersfield, Huddersfield, UK
[2.] Department of Vehicle Engineering, Taiyuan University of Technology, Shanxi, 030024, P.R. China
[3]State Key Laboratory of Mechanical Transmission, Chongqing University, P.R. China
Email: f.gu@hud.ac.uk

***Abstract*—Induction motors are the most widely used electrical machines in industry. To diagnose any possible incipient faults, many techniques have been developed. Motor current signature analysis (MCSA) is a common practice in industry to find motor faults. However, because small modulations due to faults it is difficult to quantify it in the measured signals which predominates with supply frequency, higher order harmonics and noise. In this paper a modulation signal (MS) bispectrum is investigated to detect different severities of stator faults. It shows that MS bispectrum has the capability to accurately estimate modulation degrees and suppress the random and non-modulation components. Test results show that MS bispectrum has a better performance in differentiating spectrum amplitudes due to stator faults and hence produces better diagnosis performance, compared with that of conventional power spectrum analysis.**

Keywords-Motor current signatur ; stator fault ;power spectrum; bispectrum;

I. Introduction

To maintain high production efficiency, plant condition monitoring of induction motors, primer power providers, have become a common practice. Correspondingly, many new techniques have been investigated to improve the performance of fault detection and diagnosis. Motor current signature analysis (MCSA) is a conventional approach for monitoring motors. The foundation of this technique is widely identified and has been explored extensively by several authors [1-5]. Many of the authors deal with mechanical faults, especially with the effects of broken rotor bars and eccentricities. Thomson and Morrison (2002) focused on stator fault diagnosis and presented good results and arguments. These works are a good introduction to MCSA condition-monitoring techniques and gives a clear overview of the analysis of faults.

Higher order spectra (HOS) are useful signal processing tools that have shown significant benefits over traditional spectral analyses because HOS have nonlinear system identification, phase information retention and Gaussian noise elimination properties. The application of HOS techniques in condition monitoring has been reported in [6, 7] and it is clear that multi-dimensional HOS measures can contain more useful information than traditional two-dimensional spectral measures for diagnostic purposes. Especially, Gu et al [7, 8] introduced a MS bispectrum which is more efficient in resolving the modulation process of current signals of a downstream compressors and gearboxes for diagnosing different common faults. However, these techniques have not been examined for stator fault diagnosis.

This paper provides the details of applying a MS bispectrum analysis to current signals to enhance feature components for the detection and diagnosis of the stator faults and compares it with conventional power spectrum. The bispectrum signal processing tools are then developed to characterise the current signals for identifying both the presence and magnitude of the seeded faults with different severity.

II. Electrical Motor Current Signals

As illustrated in Fig. 1 there are four typical stator faults: winding short turn, open circuit, phase-to-phase short and phase-to-ground. These asymmetric stator faults are usually related to insulation failures which are resulted from different reasons such as overloading, poor connection etc. It has reported in [1] that about 38% of all reported induction motor failures fall into these fault modes. Because of this high fault rate, stator fault diagnosis has been studied extensively and a range of papers published on the analysis of air gap, axial flux and terminal current signals to understand possible fault mechanisms for finding effective and reliable features in measured current signals.

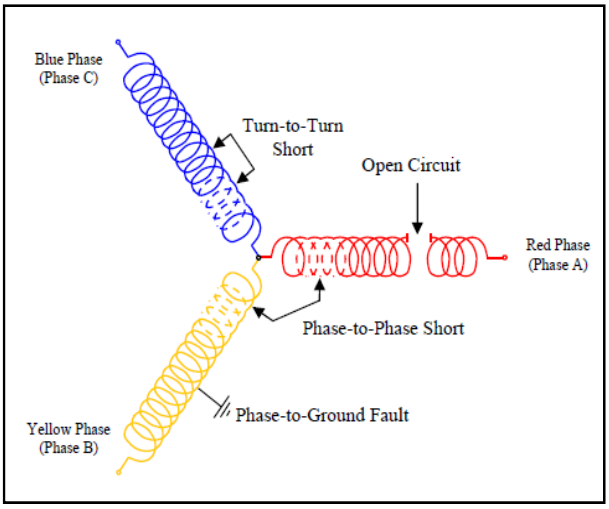

Figure 1. Different three-phase stator winding faults.

In general, stator faults causes uneven distribution of the air-gap flux waveform around the stator cross section, which makes the stator currents to be modulated by rotor slot frequency and the feature frequencies in current signals can be found at characteristic frequencies[9]:

The authors are grateful for the financial support provided by the National Natural Science Key Foundation of China under Contract No. 51035008

$$f_{sf} = f_s\left[1 \pm mN_b\left[\frac{1-s}{p}\right]\right] \quad (1)$$

To be convenient for field engineers, (1) can be expressed in terms of rotor frequency as

$$f_{sf} = f_s \pm mN_b f_r \quad (2)$$

where f_s supply frequency, f_r rotor speed, s the motor slip, N_b number of rotor bars, p number of pole-pairs and m= 1, 2, 3… is the harmonics orders.

III. Analysis techniques

A. Power Spectrum

Power spectrum method is generally used to describe the power distribution of electrical current signal in the frequency domain for obtaining diagnostic information. Usually it is calculated using Fourier transform (FT) by:

$$P(f) = E\{X(f)\, X^*(f)\} \quad (3)$$

where $X(f)$ and its conjugate $X^*(f)$ are the Fourier transform of the signal sequence $x(n)$; and *E{.} is* the expectation operator.

B. Conventional Bispectrum

The bispectrum analysis is a type of higher order spectra (HOS), which is used by a large number of researches since 1980s[10] in different fields such as communications and medicine. Given a discrete time current signal x(n), its discrete Fourier transform (DFT), X(f) is defined to be

$$X(f) = \sum_{k=-\infty}^{\infty} x(n)e^{-j2\pi fn} \quad (4)$$

Equation (4) can be written in term of magnitude |X(f)|and phase $\emptyset_f$ as

$$X(f) = |X(f)|\, e^{j\emptyset_f} \quad (5)$$

According to [11] the conventional bispectrum can be defined as

$$B(f_1, f_2) = E\{X(f_1)\, X(f_2)\, X^*(f_1 + f_2)\} \quad (6)$$

where *f1*, *f2* and *f1+ f2* indicate the individual frequency components achieved from Fourier series integral.

Bispectrum analysis has a number of unique properties such as nonlinear system identification, phase information retention and Gaussian noise elimination when compared with power spectrum analysis. Especially, bispectrum is a very effective tool for detecting quadratic phase coupling (QPC) which occurs when two waves interact non-linearly and generate a third wave with a frequency and phase equal to the sum (or difference) of the first two waves.

A summary of the various bicoherence estimators can be found in [12]. The definition of squared bicoherence used in (7) is chosen because it is bounded between 0 and 1 which is easy for comparing the degree of nonlinearity or coupling effect between different signals.

$$b^2(f_1, f_2) = \frac{|B(f_1, f_2)|^2}{E\{|X(f_1)X(f_2)|^2\}E\{|X(f_1+f_2)|^2\}} \quad (7)$$

A normalized form of the bispectrum or bicoherence is usually used to measure the degree of coupling between coupled components. The bicoherence is close to 1 if there are nonlinear interactions among frequency combinations f_1, f_2 and $f_1+ f_2$. On the other hand, a value of near 0 means an absence of interactions between the components. Therefore, based on the amplitude of bicoherence the nonlinear interactions can be detected and the interaction degrees can be also measured between the coupling components.

If the frequency components at f_1, f_2 and $f_1+ f_2$ are independent components, each frequency will be described by statistically independent random phases distributed over(-π, π). Upon statistical averaging denoted by the expectation operator *E{.}* in (6), the bispectrum will tend towards zero due to the random phase mixing effect. In this way random noise can be suppressed significantly

On the other hand, if the three spectral components: f_1, f_2 and $f_1+ f_2$ are non-linearly coupled to each other, the total phase of the three components will not be random at all, even though each of the individual phases are random, in particular, the phases have the following relationship:

$$\emptyset(f_2) + \emptyset(f_1) = \emptyset(f_2 + f_1) \quad (8)$$

Consequently, the statistical averaging will not lead to a zero value in the bispectrum. This nonlinear coupling is indicated by a peak in the bispectrum at the bifrequency $B(f_1, f_2)$.

C. Modulated MS Bispectrum

Even though conventional bispectrum representation of current signal permits the inclusion of phase information and the elimination of Gaussian noise, it produces unstable results due to random phase variation of the sideband components in the current signal.

Equation (6) includes only the presence of nonlinearity from the harmonically related frequency components: f_1, f_2 and f_1+f_2. It overlooks the possibility that the occurrence of f_1-f_2 might be due to the nonlinearity between f_1 and f_2 as well. Because of this, it is not adequate to describe amplitude modulation (AM) signals such as motor current signals.

To improve the performance of the conventional bispectrum in characterizing the motor current signals, a new variant of the conventional bispectrum, named as a modulation signal bispectrum (MSB) is examined in [7, 13] as in (9)

$$B_{MS}(f_1, f_2) = E\{X(f_2 + f_1)\, X(f_2 - f_1)\;\; X^*(f_2)\;\; X^*(f_2)\} \quad (9)$$

Furthermore, to make a direct comparison with power spectrum in (3) a normalized version of (9) can be introduced as:

$$B_{MSN}(f_1, f_2) = E\left\{X(f_2 + f_1)X(f_2 - f_1)\; \frac{X^*(f_2)}{|X(f_2)|}\frac{X^*(f_2)}{|X(f_2)|}\right\} \quad (10)$$

In (10) the amplitude of $\frac{X^*(f_2)}{|X(f_2)|}$ which relates to carrier component f_2 is unity. Thus the amplitude of MS bispectral peaks is determined purely by the magnitude effect of sideband components. In other words the resultant MS bispectral magnitudes are not influenced by the carrier component at supply frequency and hence the product of two symmetrical sidebands $|X(f_2 + f_1)X(f_2 - f_1)$ is equal to either $|X(f_2 - f_1)X^*(f_2 - f_1)$ or $|X(f_2 - f_1)X^*(f_2 - f_1)$ in (3) because the two sidebands have the same amplitudes.

However, the phase information of f_2 is still maintained. Therefore, the normalized MS bispectrum also have the noise cancellation property of bispectrum. Because of this noise cancellation, it is more accurate in estimating modulation magnitude. In contrast the magnitude of power spectrum has the contributions from noise and leads to an overestimation of sidebands components and hence less accurate diagnosis results.

IV. EXPERIMENTAL METHODS

To show the performance of MSD bispectrum in analyzing current signals, a dataset is acquired in a motor rig under different simulated fault cases and operating conditions. Fig. 2 shows the schematic diagram of the test facility employed to examine motor stator faults. The system consists of an induction motor, variable speed controller, supporting bearings, couplings and DC generator as a load. The test motor is a three-phase induction motor with rated output power of 4 kW at speed 1420 rpm (two-pole pairs) and 28 rotor bars. To change the speed of the testing motor, a digital variable speed controller is attached to the test rig between the power line source and the motor. The controller can be programmed to any specific shaft rotation speed between 0 and 1500rpm. The induction motor is directly coupled with a loading DC generator. The field of the generator is connected to DC source through controller while the generated power was fed back to the mains electrical grid and the load in the induction motor can be adjusted by changing the field resistance of the DC generator. The operating load can be varied from no load to full load via the control panel.

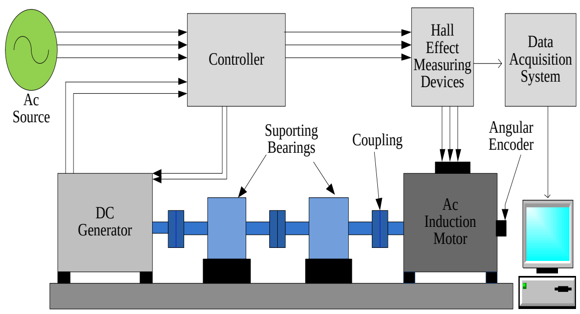

Figure 2. Schematic diagram of the induction motor test facility.

A power supply measurement unit is designed to measure instantaneous AC voltages, currents and power, using hall-effect voltage and current transducers and a universal power cell. A shaft encoder, mounted on the shaft end produces 100 pulses per revolution for measuring the motor speed.

During tests all the data was acquired using a GST YE6232B high speed data acquisition system. This system has 16 channels, each with a 24 bit analogue-digital converter at a maximum sampling frequency of 96 kHz, which allows the details of the 50Hz component, the high order supply harmonics, rotor bar pass frequency, stator bar pass frequency to be recorded for further analysis.

To evaluate the performance of MSB analysis, current signals were collected under three different stator winding configurations: healthy motor, one coil removal and two-coil removal under four successive load conditions: zero, 25%, 50% and 75% of full load, which allows the diagnostic performance to be examined at different loads and avoid any possible damages of the test system at the full load when the faults are simulated. As shown in Fig. 3, there are three parallel coils in each phase. By reconfiguring the terminals of the phase terminals, it allows rewiring the three coils in phase B in three different ways: supply to B1-B2-B3 for the healthy case, supply B1-B2 for the case of one coil removal which represents a smaller fault and supply to B1 only for two conductor removal which represents a larger fault. Obviously, these coil removals could be a simulation of asymmetric stator which will increase the motor equivalent impedance and hence degrade motor performance.

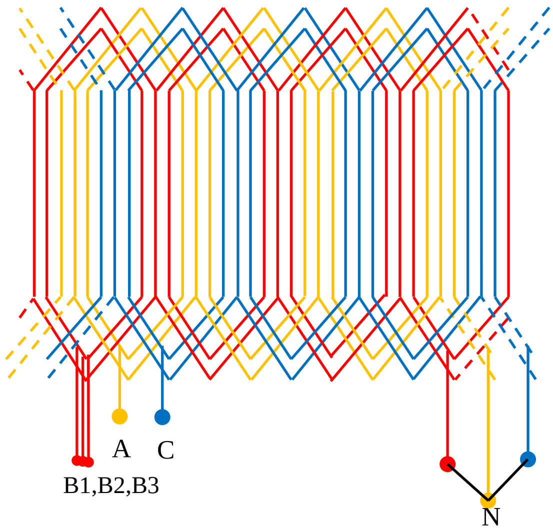

Figure 3. Shcametic of stator fault simulation in phase B

V. RESULTS AND DISCUSSIONS

The dataset is processed off-line by using a Matlab program which implements FT calculation to obtain both power spectrum using (3) and MS bispectrum using (10) simultaneously. During the calculation it uses a rectangular FT window of the same size for both power spectrum and MS bispectrum, which results in a frequency resolution of 0.125Hz, and the same average times so that they can be compared directly in their performance of identifying fault characteristic frequencies and quantifying spectral peaks. In the meantime, only the current signal in phase B is examined as the fault is induced to this phase and it produces the most significant changes between the three phases. In addition, a MSB slice only at 50Hz is presented for direct comparison because this slice gives full information about the modulation characteristics.

A. Spectrum Characteristics

Fig. 4 shows a typical MS bispectrum for current signal under 75% load when the motor is healthy. As shown in Fig.4 (b) the 50Hz supply component in power spectrum is eliminated completely in MSB. This makes easier and more reliable to examine components that relate to motor heath conditions. For example, the sideband components: (50-3.12)Hz and (50+3.12)Hz around the 50Hz shown by power spectrum of Fig. 4(b), arisen by rotor asymmetric errors, is combined into a single bispectral peak at frequency 3.12Hz, which is much easier to be identified and hence MSB allows a significant reduction of the efforts in spectrum analysis.

Moreover, MSB shows very good performance in noise reduction. Comparing it with power spectrum shown in Fig.4 (a), it can be found that the spectrum noise floor is about a 10dB lower than that of power spectrum. This makes spectral peaks such as that due to stator faults in the high frequency range to be estimated more accurately and hence to obtain more accurate and better diagnostic results.

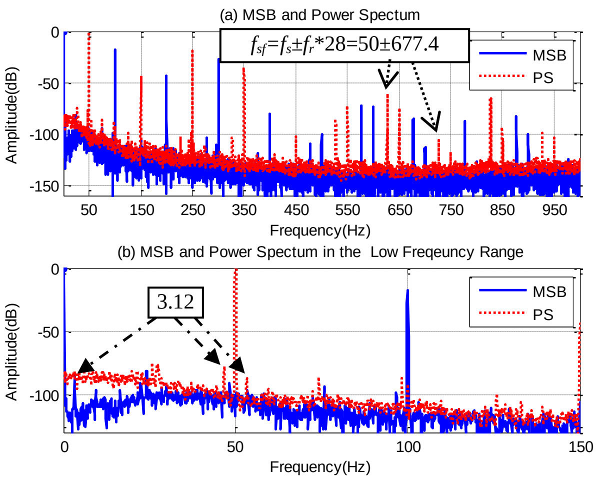

Figure 4. MSB and power spectrum characteristics

B. Stator Fault Diagnosis by Power Spectrum

Fig. 5 shows typical power spectra for the current signals collected under different loads namely zero load, 25% load, 50% load and 75% load. For the healthy case the characteristic frequency values shift lower and the peak amplitude goes higher with increasing in loads. The existence of the characteristic frequencies in the healthy case is due to evitable manufacturing tolerances or inherent errors that lead to a clear asymmetric distribution between the three stator phases.

However, as the asymmetry becomes worse due to the fault introduces the amplitude increases slightly and the frequency shifts also becomes slightly larger when comparing the results under different motor fault cases, which is consistent with that the faults result in weaker magnetic field and more rotor slip. Thus these changes may be used for separating different health cases.

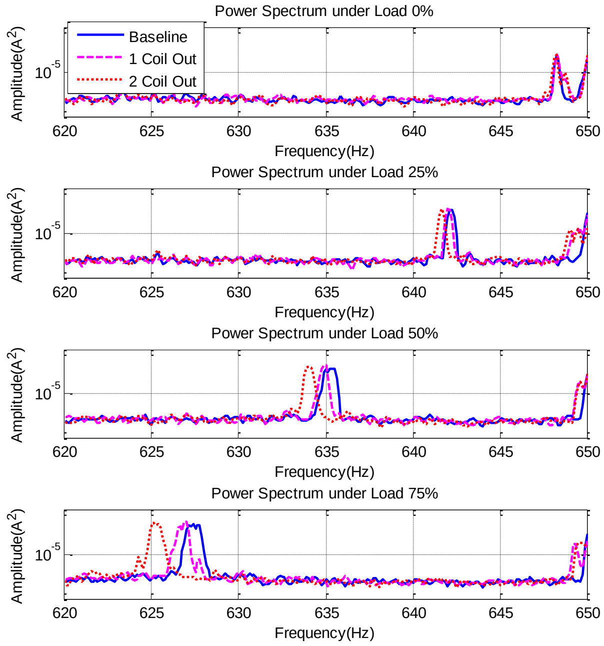

Figure 5. Current power spectrum zoomed around lower sidebands of bar-pass-frrequency under different loads and stator cases.

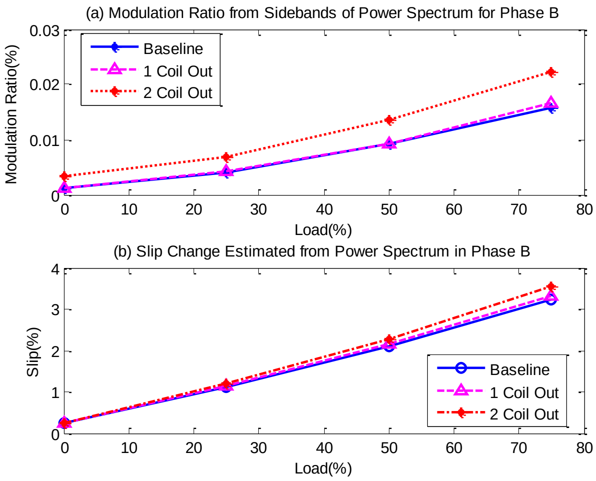

Figure 6. Diagnosis by amplitude changes and slip changes from power spectrum

Fig. 6 present the diagnostic results based on the change in the amplitude and frequency estimated from power spectrum using dataset from phase B. The modulation ratio used in Fig. 6(a) is calculated by normalizing the mean value of two sideband amplitudes with the root mean square (RMS) values of current signals whereas the slip is estimated using the frequency values extracted from power spectrum based on (1). As shown in Fig. 6, the relative amplitude change and frequency change increase with increasing in loads and fault levels, which is consistent with the operating principles of induction motors. However, these load trends makes it impossible to separate the healthy motor and the one coil removal case under load conditions below 50%. In means that a full separation can be reached only at 70% load although its difference between healthy motor and one-coil removal is very small.

In addition, the amplitude changes can give a full separation under different load conditions when it has two coil removals on the stator, which shows that amplitude changes is less sensitive to loads and can be a useful feature for power spectrum based diagnosis.

C. Stator Fault Diagnosis by MS Bispectrum

Typical stator current MS bispectra are shown in Fig.7 for the current signals from different loads and motor health cases. Similar to the characteristics observed from power spectra in Fig. 5, MSB peak amplitudes at the characteristic frequencies increases and the frequency value shifts lower as load increases. However, the amplitude increases more significantly with the progression in fault severity. In addition, bispectral peaks in Fig. 7 appear at frequency values that have a 50Hz difference from that of power spectrum, showing the effect of MSB demodulation.

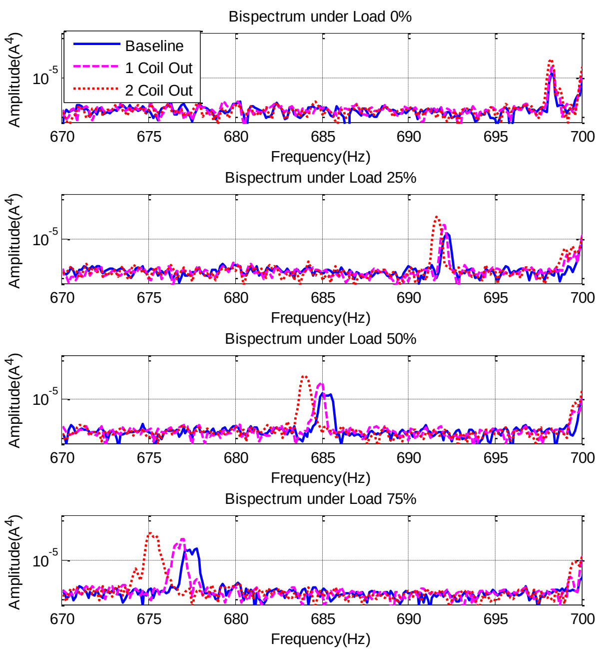

Figure 7. Current MS bispectrum under different loads and stator health cases

In the same way as that of power spectrum, the healthy case exhibits a frequency shift toward to lower value and an amplitude increase as the load increases. However, for the faulty cases, MSB amplitudes increase more significantly and the frequency shifts also becomes slightly larger as the fault severity become higher. Especially, the larger changes in amplitudes with fault cases demonstrates that MSB has very effective noise reduction which allows small amplitude to be estimated accurately and hence produce accurate modulation estimation.

To give an overall assessment of using MSB for fault diagnosis, results are presented in the same way as in power spectrum to show relative amplitude changes and frequency changes in Fig .8. Obviously, the frequency change based diagnosis of Fig.8 (b) shows the same results as that of power spectrum because both MSB and bispectrum are calculated using the same frequency resolution. However, it can be seen that the amplitude change based diagnosis show nearly full separation results, demonstrating that MSB have a much better performance in diagnosing the stators faults.

VI. CONCLUSION

MSB is evaluated using phase current signals to monitor stator faults. From its spectrum presentations, it can be found that MSB show a simpler spectrum structure compared with power spectrum. Moreover it has nearly 10dB noise reduction in the whole frequency range and produces more accurate amplitude estimation.

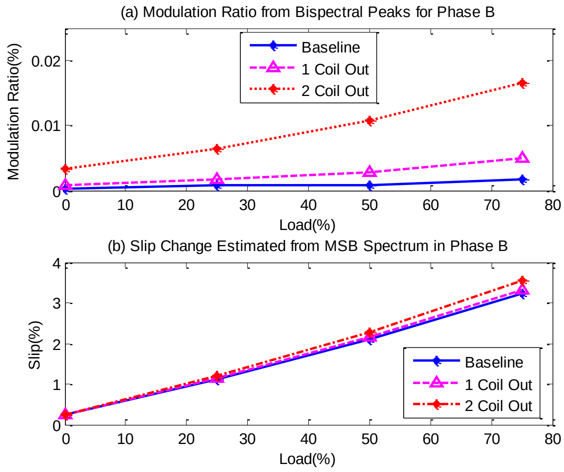

Figure 8. Diagnosis by amplitude changes and slip changes from MSB analysis

The stator fault causes the amplitude changes and frequency shifts at the characteristic frequency which can be represented by diagnostic features: modulation ratio and slip respectively. MSB modulation ratio produces a full separation of different motor cases whereas power spectrum can only separate the two-coil removal case. This shows that MSB has a better performance in diagnostic stator faults. Simultaneously, Both MSB slip and power spectrum slip values can be based on for diagnostic under high load conditions even if for the two coil removal case, showing that it perform relatively poorer and not suitable to be used as a diagnostic feature.

In the case of power spectrum, peaks appear at frequencies of ($f_s \pm N_b * f_r$) and increase as the load and fault increases as well as the sidebands shaft to the left as the fault severity increases because of changing in flux.

In a similar way, the phase current bispectrum sidebands also increase in amplitudes with load but they appear at ($N_b * f_r$). Interestingly, MS bispectrum has no modulation influences which shows the faults much clearer that makes it easier to identify and more accurate to quantify the characteristic frequency of different stator fault to produce more accurate diagnostic results.

REFERENCES

[1] W. T.Thomson and M. Fenger, "Current signature analysis to detect induction motor faults," IEEE Industry Applications Magazine pp. 26-34, 2001.

[2] W. T. Thomson and D. Morrison, "On-line Diagnosis of Stator Shorted Turns in Mains and Inverter Fed Low Voltage Induction Motors," Proceedings of IEEE Power Electronics Machines and Drives Conference, pp. 122-127, 2002.

[3] M. E. H. Benbouzid and G. B. Kliman, "What Stator Current Processing-Based Technique to Use for Induction Motor Rotor Fault Diagnosis?," IEEE Trans. Energy Convers, vol. 18, pp. 238-244., 2003.

[4] S. Nandi, H. AToliyat, and X. D. Li, "Condition Monitoring and Fault diagnosis of ElectricalMotors- A Review," IEEE Trans. Energy Convers, vol. 20, pp. 719-729, 2005.

[5] A. Alwodai, F. Gu, and A. Ball, "Motor Current Signature Analysis of a Variable Speed Drive for Motor Fault Diagnosis," Proceedings of the 24th COMADEM2011, pp. 884–892, 2011.

[6] N.Arthur and J.Penman, "Induction machine condition monitoring with higher order spectra," IEEE Transactions on Industrial Electronics, vol. 47, pp. 1031–1041, 2000.

[7] F. Gu, Y. Shao, N. Hu, and A. D. Ball, "Electrical motor current signal analysis using a modified bispectrum for fault diagnosis of downstream mechanical equipment," Mechanical Systems and Signal Processing vol. 25, pp. 360–372, 2011.

[8] M. Haram, T. Wang, F. Gu, and A. Ball, "An Investigation of the Electrical Response of A Variable Speed Motor Drive for Mechanical Fault Diagnosis " Proceedings of the 24th International Congress on Condition Monitoring and Diagnostic Engineering Management (COMADEM 2011). pp. 867-874, 2011.

[9] J. Cusidó, L. Romeral, J. A. Ortega, A. Garcia, and J. Riba, "Signal Injection as a Fault Detection Technique," Sensors, vol. 11, pp. 3356-3380, 2011.

[10] G. C. Zhang, M. Ge, H. Tong, Y. Xu, and R. Du, "Bispectral analysis for on-line monitoring of stamping operation," Engineering Applications of Artificial Intelligence, vol. 15, pp. 97–104, 2002.

[11] W.B.Collis, P.R.White, and J.K.Hammond, "Higher-orderspectra:thebispectrumandtrispectrum," MechanicalSystemsandSignalProcessing, vol. 12, pp. 375–394, 1998.

[12] J. W. A. Fackrell, S. McLaughlin, and P. R. White, "Bicoherence estimation using the direct method. Part 1: Theoretical considerations," Appl. Signal Process, vol. 3, pp. 155–168, 1995.

[13] J. R. Stack, R. G. Hartley, and T. G. Habetler, "An amplitude modulation detector for fault diagnosis in rolling element bearings," IEEE Transactions on Industrial Electronics vol. 51 pp. 1097–1102, 2004.